Inhibition of de novo ceramide biosynthesis by FTY720 protects rat retina from light-induced degeneration[S]

Hui Chen,[*,§,] Julie-Thu A. Tran,[*,§] Annette Eckerd,[*,§] Tuan-Phat Huynh,[*,§] Michael H. Elliott,[*,†,§] Richard S. Brush,[*,§] and Nawajes A. Mandal[1,*,†,§]**

Departments of Ophthalmology* and Physiology,[†] University of Oklahoma Health Sciences Center, Oklahoma City, OK 73104; Dean McGee Eye Institute,[§] Oklahoma City, OK 73104; and Ophthalmology Department,** Sichuan Academy of Medical Sciences & Sichuan Provincial People's Hospital, Chengdu City, Sichuan, 610072, China

Abstract **Light-induced retinal degeneration (LIRD) in albino rats causes apoptotic photoreceptor cell death. Ceramide is a second messenger for apoptosis. We tested whether increases in ceramide mediate photoreceptor apoptosis in LIRD and if inhibition of ceramide synthesis protects the retina. Sprague-Dawley rats were exposed to 2,700 lux white light for 6 h, and the retinal levels of ceramide and its intermediary metabolites were measured by GC-MS or electrospray ionization tandem mass spectrometry. Enzymes of the de novo biosynthetic and sphingomyelinase pathways of ceramide generation were assayed, and gene expression was measured. The dosage and temporal effect of the ceramide synthase inhibitor FTY720 on the LIRD retina were measured by histological and functional analyses. Retinal ceramide levels increased coincident with the increase of dihydroceramide at various time points after light stress. Light stress in retina induces ceramide generation predominantly through the de novo pathway, which was prevented by systemic administration of FTY720 (10 mg/kg) leading to the protection of retinal structure and function. The neuroprotection of FTY720 was independent of its immunosuppressive action. We conclude that ceramide increase by de novo biosynthesis mediates photoreceptor apoptosis in the LIRD model and that inhibition of ceramide production protects the retina against light stress.**—Chen, H., J-T. A. Tran, A. Eckerd, T-P. Huynh, M. H. Elliott, R. S. Brush, and N. A. Mandal. **Inhibition of de novo ceramide biosynthesis by FTY720 protects rat retina from light-induced degeneration.** ***J. Lipid Res.*** **2013.** 54: **1616–1629.**

Supplementary key words light-induced retinal degeneration • photoreceptor • apoptosis • fingolimod • sphingomyelinase

Apoptotic photoreceptor cell death is the hallmark of major retinal degenerative diseases, including retinitis pigmentosa and age-related macular degeneration (1–3). Very few effective therapies exist for this heterogeneous group of diseases because of the complex pathophysiology associated with genetic and environmental factors. Researchers are looking for cellular second messengers involved in the process of cell death which can be targeted for therapies. The sphingolipid metabolite ceramide is a deadly second messenger in the cell and can induce apoptosis through various mechanisms (4). Recently, increases in ceramide levels have been shown to be associated with photoreceptor and retinal pigment epithelium (RPE) cell death (5–8). Here we investigated whether ceramide is involved in photoreceptor cell death in light-induced retinal degeneration (LIRD).

LIRD is a useful model for studying the mechanism of photoreceptor cell death because intense light exposure induces oxidative stress-mediated apoptosis of photoreceptor cells and causes retinal degeneration (3, 9). Since its development in 1966 by Noell et al. (10), this model, in combination with genetic knock-out models (1–3, 11–14), has been extensively used to discover many fundamental mechanisms of photoreceptor function and to test various neuroprotective compounds (15–21).

However, the precise mechanism of light-induced retinal degeneration is currently unclear (3, 13). In past decades, accumulating evidence suggested that ceramide, the core lipid of sphingolipid metabolism, is a key factor in apoptotic cell death (4, 22–25). Various external stressors, such as hypoxia, chemotherapeutic agents, heat, ultravio-

This work was supported by grants from the National Center for Research Resources (Grant RR-17703), the National Eye Institute (Grants EY-022071, EY-021725, and EY-019494), the Knights Templar Eye Foundation, Inc., University of Oklahoma College of Medicine Alumni Association, Foundation Fighting Blindness, Research to Prevent Blindness, Inc. USA, and National Natural Science Foundation of China (81271035/H1205).

Manuscript received 16 December 2012 and in revised form 2 March 2013.

Published, JLR Papers in Press, March 6, 2013
DOI 10.1194/jlr.M035048

Abbreviations: aSMase, acidic sphingomyelinase; CerS, ceramide synthase; dh-Sph, dihydrosphingosine; ER, endoplasmic reticulum; ERG, electroretinography; ESI-MS/MS, electrospray ionization tandem mass spectrometry; IS, internal standard; LIRD, light-induced retinal degeneration; nSMase, neutral sphingomyelinase; ONH, optic nerve head; ONL, outer nuclear layer; RPE, retinal pigment epithelium; S1P, sphingosine-1-phosphate; Sph, sphingosine; Sphk, sphingosine kinase; SPT, serine palmitoyl transferase.

[1]To whom correspondence should be addressed.
e-mail: mmandal@ouhsc.edu

[S] The online version of this article (available at http://www.jlr.org) contains supplementary data in the form of one table.

let radiation, and lipopolysaccharides, have been shown to increase intracellular ceramide levels and to signal for cell death (26). The earliest connection between ceramide and photoreceptor apoptosis was described in Drosophila models of photoreceptor degeneration in which decreasing ceramide levels prevented photoreceptor apoptosis (27). We hypothesized that light stress can induce ceramide increases in the retina to activate apoptotic photoreceptor cell death, and that blocking this ceramide increase will protect photoreceptors against light stress. Myriocin and fumonisin 1B are the most-common de novo ceramide biosynthetic inhibitors, but they are highly toxic. We searched for a compound with less in vivo toxicity that could be delivered systemically, and found FTY720, which was derived from myriocin, to reduce its toxicity (28). FTY720 has been tested through three phases of human clinical trials for relapsing multiple sclerosis due to its immunosuppressive properties (29–32). FTY720 is a structural analog of sphingosine (Sph); the mechanism of action of FTY720 as deciphered in MS studies is through its phosphorylation to FTY720-P by sphingosine kinase 2 (Sphk2), similar to Sph conversion to sphingosine-1-phosphate (S1P). As a mimic of S1P, FTY720-P modulates S1P receptor signaling in lymphocyte homing and trafficking and thus acts as an immunosuppressor for MS (33, 34). FTY720 was recently reported to inhibit Cer synthase (CerS) and to block de novo Cer production (35, 36). We used our light-stress model of albino rats to determine whether FTY720 can inhibit ceramide generation in light-stressed retinas. FTY720 has been used in several animal models, including rodent models of experimental autoimmune uveitis, due to its immunosuppressive properties (37–39). Its safety in animal and human uses and its ability to cross the blood-brain barrier have been well documented (30, 32, 40).

In the current study, we established that retinal ceramide levels increased in the LIRD retinas before the onset of photoreceptor apoptosis and that systemic delivery of FTY720 effectively prevented ceramide increases in the retina and protected photoreceptors from apoptotic cell death.

EXPERIMENTAL PROCEDURES

Animals and materials

All procedures were performed according to the Association for Research in Vision and Ophthalmology (ARVO) Statement for the Use of Animals in Ophthalmic and Vision Research and the University of Oklahoma Health Sciences Center Guidelines for Animals in Research. All protocols were reviewed and approved by the Institutional Animal Care and Use Committees of the University of Oklahoma Health Sciences Center and the Dean A. McGee Eye Institute. Sprague-Dawley albino rats (both male and female) were born and raised in dim cyclic light (5–10 lux; 12 h dark/12 h light) until they were used in experiments. FTY720 was purchased from Selleck Chemicals (Houston, TX).

Light damage of Sprague-Dawley rats and treatment with FTY720

Eight-to-ten-week-old rats were exposed to damaging light (white cool light) for 6 h (9 AM to 3 PM) at an intensity of 2,700 lux. After light damage, the rats were returned to their native dim cyclic room, and retinas to be used for RNA, protein, and lipid analysis and eyes to be used for cryosectioning were collected at different time points following exposure. Retinas were harvested by "Winkling" as described by Winkler (41) and snap frozen in liquid nitrogen. For cryosections, rat eyeballs were fixed in 4% paraformaldehyde and embedded in Tissue Tek® OCT, and 10 μm cryosections were prepared for immunolocalization studies. For intraperitoneal injection, FTY720 (Selleck Chemicals; Houston, TX) was dissolved in a vehicle containing sterile DMSO (100%) (Sigma; St Louis, MO) and saline (0.9%) 1:1 (v/v). A dose response was determined using 2.5, 5.0, and 10.0 mg of FTY720/kg of body weight injected 0.5 h before the start of light exposure. We tested a treatment of three doses of 2.5 mg/kg FTY720 at 16 h before, 0.5 h before, and immediately (0 h) after the 6 h-long light damage. A temporal effect was tested using a single dose of 10 mg of FTY720/kg body weight administered at several time points (16 h, 24 h, 48 h) before light exposure and immediately (0 h) after exposure.

Electroretinography

After light exposure, rats were returned to dim cyclic light (5–10 lux) for 7 days before electroretinography (ERG) recordings were performed. Flash ERGs were recorded with the Diagnosys Espion E2 ERG System (Diagnosys, LLC; Lowell, MA) as described in previous publications (15, 16). For the assessment of rod photoreceptor function (scotopic ERG), four strobe flash stimuli were presented at flash intensities of −2.3, −1.3, 0.7, and 2.7 log cd.s/m^2. The amplitude of the a-wave was measured from the prestimulus baseline to the a-wave trough at the highest light intensity. The amplitude of the b-wave was measured from the trough of the a-wave to the peak of the b-wave.

Possible defects in the visual cycle were analyzed by measuring the time course of dark adaptation (recovery of rod photoreceptor sensitivity) following a bleaching light exposure. Rats were fully dark-adapted and injected intraperitoneally with FTY720 (10 mg/kg) or vehicle (50% DMSO). Full-field scotopic ERGs for both eyes were recorded for a single test flash of 2.3 log cd.s/m^2 10 min after injection of FTY720. Rats were then exposed to a steady field of log 2.3 cd.s/m^2 for 2 min in the Ganzfeld dome to bleach rod photoreceptors. Immediately following the bleaching period (time = 0 min), and every 10 min thereafter (time = 10, 20, 30, 40, 50, 60, 70, and 80 min), the same test flash of 2.3 log cd.s/m^2 was presented. The a-wave responses at the indicated times after bleaching were normalized to the initial dark-adapted response for each rat.

Histology

After ERG recordings, rats were euthanized by carbon dioxide asphyxiation for light microscopic evaluation of retinal structure following previously published methods (15, 16). In brief, eyes were harvested and marked with a tattoo dye at the 12 o'clock position on the limbus and fixed. Five micron-thick sections were cut along the vertical meridian through the optic nerve head (ONH). On hematoxylin and eosin-stained sections, the thickness of the outer nuclear layer (ONL) was measured at 0.5 mm distances from the center of the ONH to the inferior and superior ora serrata and plotted as a spider diagram.

Apoptosis detection by terminal deoxynucleotidyl transferase dUTP nick end labeling assay

DNA fragmentation as an earlier marker of apoptosis was determined by terminal deoxynucleotidyl transferase dUTP nick end labeling (TUNEL) assay using a commercial kit from Takara (Clontech; Mountain View, CA). Frozen sections of rat retina harvested at different time points after light damage were used

for the assay, along with controls that were not light damaged. Fluorescent signals were imaged on an Olympus Fluoview FV500 confocal microscope.

Quantitation of rhodopsin

To measure the effect of FTY720 on the rate of rhodopsin regeneration, dark-adapted rats were injected intraperitoneally with FTY720 (10 mg/kg) or vehicle 0.5 h prior to a 1 h bleach in room light (~400 lux). Immediately following the bleach (time = 0 min), a group of FTY720- and vehicle-treated rats were euthanized, and retinas were removed and snap frozen. The remaining rats were dark-adapted and retinas were collected under dim red light at 1, 2, 3, and 6 h after the bleach. An additional group of rats was dark-adapted overnight, injected with FTY720 or vehicle, and maintained in darkness for 2 h to serve as dark-adapted controls and to determine if FTY720 had a direct effect on the binding of chromophore to rhodopsin.

Rhodopsin measurements were performed as described previously (15, 42). Briefly, under dim red light, each retina was homogenized in 400 μl of buffer containing 10 mM Tris-HCl (pH 7.4), 150 mM NaCl, 1 mM EDTA, 2% (w/v) octylglucoside, and 50 mM hydroxylamine. Homogenates were centrifuged at 16,000 *g*, and soluble lysates were scanned from 270–800 nm in a spectrophotometer (Ultrospec 3000 UV/Vis Spectrophotometer; GE Healthcare, Piscataway, NJ). Samples were then bleached under room light for 10 min and scanned again. The difference spectra at 500 nm between pre- and postbleached samples were used to determine rhodopsin content using a molar extinction coefficient of 42,000 M^{-1} (43). The data are presented as rhodopsin content/retina.

GC-MS quantification of cellular free ceramide

Total lipids were extracted from frozen retinas using the Bligh and Dyer method, and free ceramides were isolated using methods described by Zhang et al. (44). An internal standard (IS) (1.0 μg C17 ceramide) (Matreya; Pleasant Gap, PA) was added to the chloroform extract of total lipids, and the lipids were applied to solid-phase extraction cartridges (100 mg Extract-Clean Silica, Alltech; Deerfield, IL) saturated with chloroform. Free ceramides were eluted with 2.5 ml of chloroform-methanol (98:2, v/v) (Fraction 2) after the neutral lipids had been eluted with 2 ml of chloroform (Fraction 1). The remaining lipid was then eluted twice with 2 ml of chloroform-methanol (1:1, v/v) to the Fraction 1. Fraction 2 containing free ceramide was dried under nitrogen and derivatized with 1% trimethylchlorosilane in *N,O* bis (trimethylsilyl) trifluoroacetamide and analyzed by GC-MS (Agilent Technologies 6890N gas chromatograph with 5975B inert XL EI/CI mass selective detector, 7683B injector, and Agilent Technologies HP-5MS 30 m × 0.25 mm × 0.25 μm column) with electron impact ionization in selected ion monitoring (SIM) mode. External standards containing serially diluted known amounts of C16, C17, C18, and C24 ceramide were processed and analyzed in a similar fashion. The analytes of interest were monitored as follows: *m/z* 311 and 370 for C16 ceramide; *m/z* 311 and 384 for C17 ceramide; *m/z* 311 and 398 for C18 ceramide; and *m/z* 311 and 482 for C24 ceramide. The peaks were quantified by comparison to external standards.

Fraction 1, which contains total lipids minus the free ceramides, was subjected to strong acid hydrolysis (16% HCl in methanol, 70°C, 4 h) and the FA methyl esters generated were analyzed by GC-flame ionization detector (45, 46). This analysis provided the nanomole and microgram values of total FAs used to normalize the samples.

Electrospray ionization tandem mass spectrometry analysis of cellular sphingolipids

Electrospray ionization tandem mass spectrometry (ESI-MS/MS) analysis of endogenous sphingosine bases (Sph), S1Ps, and ceramide species was performed on a Thermo-Fisher TSQ quantum triple quadrupole mass spectrometer, operating in a multiple reaction monitoring positive-ionization mode, using a modified version of a previously published protocol (47). Briefly, 1–2 retinas/sample were homogenized and extracted with ethyl acetate-isopropanol-water (60:30:10) after being fortified with the ISs C_{17} base D-erythro-sphingosine (17CSph), C_{17} sphingosine-1-phosphate (17CSph-1P), *N*-palmitoyl-D-erythro-C_{13} sphingosine (13C16-ceramide), and heptadecanoyl-D-erythro-sphingosine (C17-ceramide). After evaporation and reconstitution in 100 μl of methanol, samples were injected on the HP1100/TSQ quantum LC/MS system, and gradient was eluted from the BDS (Base Deactivated Silica) Hypersil C8 (150 × 3.2 mm × 3 μm particle size) column with 1.0 mM methanolic ammonium formate mobile-phase system. Ceramide, Sph, and S1P peaks were identified based on retention time and mass fragments. Peaks corresponding to the target analytes and IS were collected and processed using the Xcalibur software system. These analyses were carried out at the lipidomics core at the Medical University of South Carolina in Charleston, SC.

Quantitative analysis was based on the calibration curves generated from external standards with known amounts of the target analyte synthetic standards and an equal amount of the IS. The target analyte/IS peak area ratios were plotted against analyte concentration. The target analyte/IS peak area ratios from the samples were similarly normalized to their respective ISs and compared with the calibration curves using a linear regression model. Finally, the quantity of the sphingolipid species was normalized with the content of inorganic phosphate (represents phospholipids) in the extracted lipid.

Gene expression analysis by quantitative RT-PCR

RNA was isolated and purified from frozen rat tissues using PureLink™ Micro-to Midi Total RNA Purification System from Invitrogen (Carlsbad, CA) following the manufacturer's protocol. Equal quantities (1.0 μg) of total RNA from each tissue were converted to first-strand cDNA using SuperScript III First-Strand Synthesis SuperMix (Invitrogen) for RT-PCR. First-strand cDNA was used for quantitative RT-PCR (qRT-PCR). Primers for qRT-PCR were designed in such a way that they spanned at least one intron, which eliminated the chance of amplification from residual genomic DNA contamination. Sequences of the primers may be obtained from the corresponding author upon request. Quantitative PCR and melt-curve analyses were performed using iQ SYBR Green Supermix (Bio-Rad; Hercules, CA) and an iCycler machine. Relative quantities of expression of the genes of interest in different samples were calculated by the comparative Ct (threshold cycle) value method (16, 48–50).

Immunohistochemistry

Immunolabeling of frozen sections was performed as described previously (49–52) using a monoclonal anti-ceramide antibody (Sigma-Aldrich; St. Louis, MO). Frozen sections were thawed, rehydrated, and treated with 1% NaBH4 to reduce autofluorescence. Nonspecific labeling was blocked using 10% normal goat serum + 5% BSA + 1% fish gelatin + 0.5% Triton X-100 in PBS ("blocker"). Excess blocker was removed, and primary antibody was applied overnight at 4°C. Sections were rinsed and incubated in anti-mouse secondary antibody (Sigma-Aldrich) conjugated to FITC (diluted 1:200 in blocker; Sigma-Aldrich) for 1 h at room temperature to visualize labeling. Sections were rinsed and cover-slipped with ProLong Gold antifade reagent with 4, 6-diamidino-2-phenylindole (DAPI) (Invitrogen). Substituting normal mouse serum for mouse monoclonal primary antiserum or omission of primary antiserum eliminated immunolabeling, indicating that labeling methods produced only specific labeling.

Confocal microscopy was performed using an Olympus FluoView FV500 microscope (Olympus Microsystems; Center Valley, PA). To ensure quantitative image quality, laser power, pinhole settings, photomultiplier tube settings, and intensity thresholds were kept constant for each retinal section imaged.

Assay for serine palmitoyltransferase activity

Serine palmitoyl transferase (SPT) (EC 2.3.1.50) is the rate-limiting and the first committed enzyme of ceramide biosynthesis that catalyzes the condensation of palmitoyl CoA and L-serine to produce 3-ketosphinganine. The SPT activity was measured based on the conversion of water-soluble [^{3}H]serine to the chloroform-soluble product 3-ketosphinganine using the protocol developed by Williams, Wang, and Merril (53), with some modification as described by Dickson, Lester, and Nagiec (54). A sample containing 400 μg of retinal protein was incubated with 300 μl reaction buffer containing 100 mM HEPES (pH 8.3), 5 mM DTT, 2.5 mM EDTA, 50 μM pyridoxal phosphate, 200 μM palmitoyl CoA, 2 mM L-serine (cold), and 1 mM [^{3}H] L-serine (specific activity: 10–30 mCi/mmol) for 30 min at 37°C with intermittent shaking. The reaction was terminated by 1.5 ml of chloroform-methanol (1:2, v/v), followed by the addition of 25 μg of carrier sphinganine, alkalization with 2.0 ml 0.5 N NH_4OH, and 1 ml chloroform. Two phases were generated by centrifugation, and the lower chloroform phase was washed twice with water and counted in a scintillation counter. SPT activity was determined from the picomoles of product formed/min/mg of protein.

Assays for acidic and neutral sphingomyelinase activity

Acidic and neutral sphingomyelinase (aSMase and nSMase) activity was indirectly measured in the retinal protein using the Amplex Red sphingomyelinase assay kit from Invitrogen. Retinas were homogenized in T-PER buffer (Pierce; Rockford, IL) with protease inhibitor cocktail and centrifuged at 17,000 *g* for 10 min at 4°C. The protein concentration in the supernatant fraction was measured with the BCA protein assay (Pierce), and the activity of aSMase and nSMase was determined by modulating the pH of the reaction buffer and following the manufacturer's protocol. Fluorescence intensity was measured at 30 min for aSMase activity and at 30 and 60 min for nSMase at 590 nm (excitation at 540 nm) using a FLUOstar Omega 96-well plate reader (Cary, NC).

Counting lymphocyte numbers

Two to four milliliters of blood was collected from rats by cardiac puncture immediately after euthanasia by carbon dioxide asphyxiation. Complete white count was obtained from a local veterinary diagnostic lab (Vance Veterinary Clinic; Oklahoma City, OK).

Statistical analyses

Statistical analyses were performed using GraphPad Prism 5.0 software (GraphPad Software, Inc.; La Jolla, CA). The quantitative data are expressed as mean ± SE for each group. One-way or two-way ANOVA and Student's and paired *t*-tests were performed to assess differences between means.

RESULTS

Light stress increases ceramide content in the retina

Continuous exposure of albino rats to intense visible light causes synchronous photoreceptor cell death by apoptosis (1–3, 55). The pyknosis of nuclei and DNA fragmentation usually begins 8–12 h after the 6 h period of light exposure at 2,700 lux intensity (15, 16, 56, 57) and eventually results in complete loss of photoreceptor cells from the central superior retina within 7 days (15, 16, 20, 58, 59). We measured retinal free ceramide levels at different time points after light damage prior to (0 h, 3 h, and 6 h after exposure) and after the onset of apoptosis (12 h, 24 h, 48 h). Quantitative GC-MS analysis of three ceramide species [C16 + C18 + C24, which constitutes >80% of retinal ceramides (45)] showed a significant increase in cellular free ceramide content in the light-stressed retina from 3 h to 24 h after exposure, with the maximum increase (∼2-fold) at 6 h after exposure (**Fig. 1A**). We further analyzed retinal levels of all the ceramide species up to 26 carbons by a more-sensitive ESI-MS/MS method. Six hours after light stress, the level of most ceramide species as well as total ceramide had increased significantly (Fig. 1B).

The upregulation of ceramide was further verified on retinal sections using monoclonal anti-ceramide antibody. In retinas incubated with anti-ceramide antibody preabsorbed with a mixture of ceramide, no labeling was detected (Fig. 1C). In control retinas not exposed to damaging light, ceramide labeling was very low and barely detected (Fig. 1D). However, the intensity of fluorescence labeling increased in the light-damaged retina in almost all the layers, with specific increased labeling in the photoreceptor and RPE layers (Fig. 1E, arrowheads).

Pathway of ceramide generation in light-induced retina

Cellular ceramide accumulation occurs through two major but distinct pathways (60). The first is the de novo biosynthesis pathway, which initiates in the endoplasmic reticulum (ER) by condensing L-serine and palmitoyl-CoA by SPT, generating dihydrosphingosine (dh-Sph), followed by acylation of dh-Sph to dihydroceramide by one of the six known CerSs (**Fig. 2**). The final reaction by dihydroceramide desaturase creates a double bond at positions 4–5 to produce ceramide (60). The second pathway is the sphingomyelinase pathway, which produces ceramide by hydrolyzing the most-abundant sphingolipid in cells, sphingomyelin, by sphingomyelinases (SMases) on the cell membrane or in lysosomal compartments (Fig. 2).

Gene expression assays

To identify the mechanism or pathway of ceramide generation in the light-stressed retina, we investigated changes in gene expression and the activity of major ceramide biosynthetic enzymes. We performed a detailed gene expression analysis of the ceramide metabolic genes (Fig. 2) by qRT-PCR in light-stressed retinas harvested at 0, 3, 6, 12, 24, and 48 h. We observed that expression of genes involved in de novo biosynthesis of ceramide, such as *CerS4* (*Ceramide synthase 4)*, increased significantly (>3-fold) at 0 h after light stress (data not shown), and that both *Spt2* (*Serine-palmitoyl transferase 2;* >4-fold) and *CerS4* (>3-fold) were upregulated significantly 6 h after light damage (**Fig. 3A**). The expression of *Sphk1* (*Sphingosine kinase 1)* was significantly higher (4–5-fold) immediately and 6 h after light damage (Fig. 3A).

RPE cells play a crucial role in photoreceptor survival and ceramide signaling in the RPE, and RPE stress may

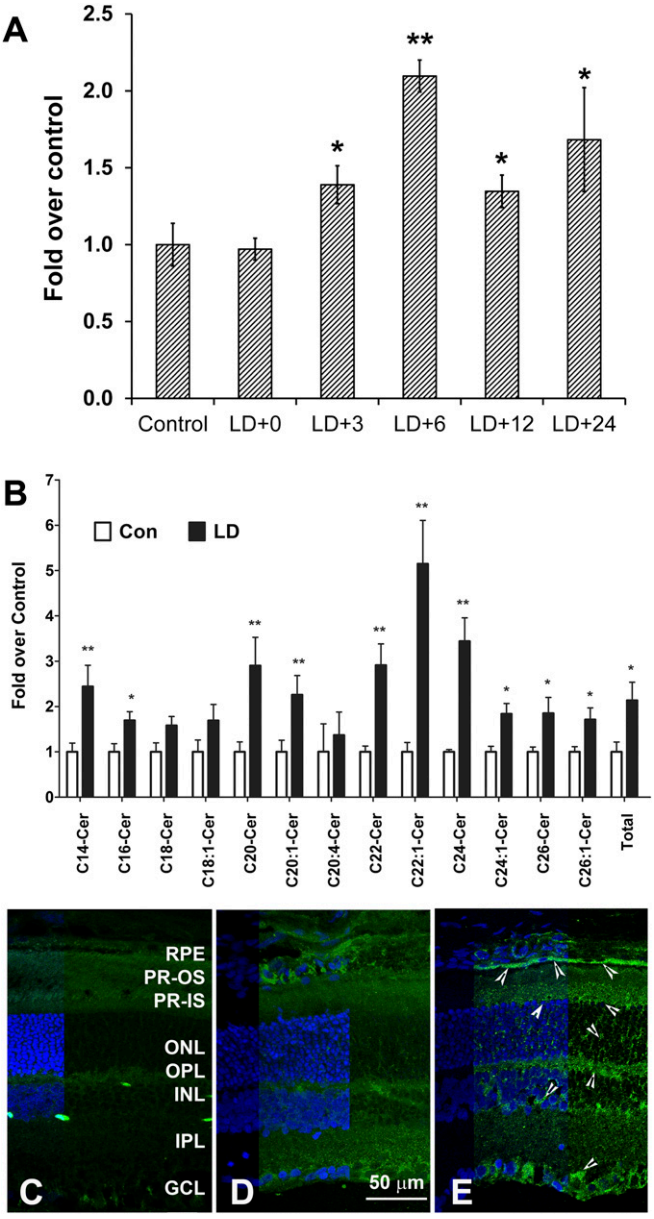

Fig. 1. Ceramide levels increase in the retina after light stress. Retinas were harvested at different time points after light damage with 2,700 lux light for 6 h. LD+0, LD+3, LD+6, LD+12 and LD+24 represent samples harvested at 0 h, 3 h, 6 h, 12 h, and 24 h after light damage, respectively. A: Retinal free ceramide levels (C16+C18+C24) were measured by GC-MS analysis and presented as fold over control retinas (no light-damaged retina) (mean + SE, n = 6). (* $P < 0.01$; ** $P < 0.001$; Student's *t*-test, statistical significance are by comparison to the first bar on the left). B: Various species of ceramides were measured by ESI-MS/MS from the retina harvested at 6 h after light damage and presented as fold over control retinas (no light-damaged retina) (mean + SE, n = 4). (* $P < 0.01$; ** $P < 0.001$; Student's *t*-test). Cryosections prepared from control (no light-damaged) (C, D) and light-damaged (E) retina. Retinal section labeled with preabsorbed antibody shown in C and without preabsorption in D and E; ceramide labeling intensity increased in light-damaged retina (E, arrowheads) in all the retinal layers. RPE, retinal pigment epithelium; PR, photoreceptors; OS, outer segments; IS, inner segments; ONL, outer nuclear layer; OPL, outer plexiform layer; INL, inner nuclear layer; IPL, inner plexiform layer; GCL, ganglion cell layer.

also be important for photoreceptor cell death. Our results show prominent ceramide immunoreactivity in the RPE following light stress (Fig. 1C). Because "winkled" retinas may contain some detached RPE cells, we assayed for the expression of the RPE-specific RPE65 gene in retinas and found 2.9–5.7% of RPE65 expression comparing to the corresponding eye cups in non-light-damaged samples. In light-damaged retinas, the level of RPE65 mRNA was not significantly different from those in non-light-damaged retinas. Although a small amount of RPE material is probably present in our retinal dissections, it is unlikely to significantly contribute to the measured increases in ceramide levels in light-damaged retinas, as whole retinas were used for lipid extraction and the modest 3–6% of RPE cells in that tissue pool is a very small fraction with respect to the neuroretinal cells.

When we analyzed expression of major genes in rat eye cups at two time points (0 h and 12 h) after light stress, we found that at 0 h after light damage, there were no major changes in the expression of any of the genes tested in the retina; however, in both retina and eyecup, the expression of almost all of the ceramide metabolic genes, including RPE65 (~2-fold), decreased significantly after 12 h, the time point at which most of the photoreceptor cells entered apoptosis (data not shown).

Activity of SPT, nSMase, and aSMase enzymes

Although gene expression studies provided some indication of the proteins induced in light-stressed retinas that resulted in increased ceramide production, there also may be changes in enzyme activity that may not be predicted by gene expression assays. We therefore measured the activity of three major enzymes involved in ceramide metabolism. Activity of the first committed enzyme of de novo ceramide biosynthesis, SPT, was increased by 20% immediately after light damage and by 50% 6 h after damage (Fig. 3B). We also observed a slight increase (~20%) in nSMase activity 3 h after damage (Fig. 3C). Interestingly, we found significant reduction in the activity of aSMase at all time points after exposure (Fig. 3D). Acid SMase (*aSMase*) is the major SMase in the retina, with mRNA expression 20–50-fold higher than neutral SMase (*nSMase*) (Mandal et al., unpublished observations). Blockage of this enzyme activity could be related to a cellular protective mechanism that reduces any further production of ceramide from sphingomyelins. However, the mechanism by which this enzyme is regulated in the retina is not known.

In summary, our gene expression and enzyme activity data suggest that de novo ceramide biosynthesis, as well as the break-down of SM specifically by nSMase, could be the probable pathways for increased levels of retinal ceramides in the light-stressed retina (Fig. 2).

Quantification of intermediary metabolites of ceramide synthesis

Of the major pathways that generate ceramide, it is the de novo pathway that generates dh-Sph and dihydroceramide, not the SMase pathway (Fig. 2). We, therefore, measured the level of these intermediates by ESI-MS/MS in light-stressed

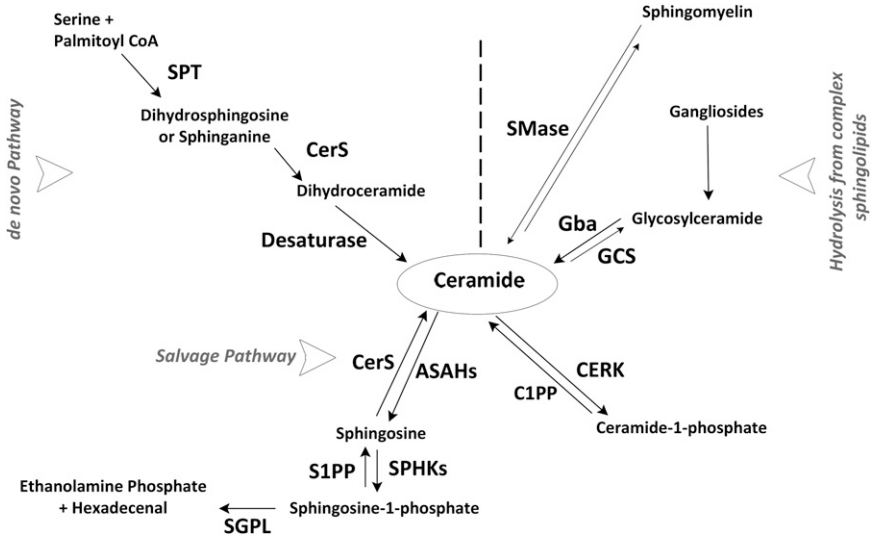

Fig. 2. Ceramide metabolic pathways in mammalian cells. Here we constructed a simplified pathway of ceramide metabolism in the cell. Ceramides are the simplest sphingolipids and are at the center of sphingolipid metabolism. There are two major pathways for ceramide synthesis in a cell: de novo biosynthesis and hydrolysis from complex sphingolipids. Also shown in the figure is the ceramide catabolic pathway, along with specific enzymes, expression of which has been studied. SPT, serine palmitoyl transferase; CerS, ceramide synthase; SMase, sphingomyelinase; Gba, glucosidase, β, acid; GCS, glucoceramide synthase; ASAHs, acyl-sphingosine amidohydrolases (ceramidases); SPHKs, sphingosine kinases; S1PP, sphingosine-1-phosphate phosphatase; SGPL, sphingosine-1-phosphate lyase; CERK, ceramide kinase; C1PP, ceramide-1-phosphate phosphatase.

retinas. The levels of both dh-Sph and dihydroceramide were significantly higher in light-stressed retinas (Fig. 3E). The level of sphingosine, which is produced from the hydrolysis of ceramide and participates in ceramide formation in the salvage pathway (Fig. 2), is not changed in the light-stressed retina (Fig. 3E). The cellular level of S1P also increased by 2-fold (Fig. 3E), which could be related to the increase in expression of the *Sphk1* gene (Fig. 3A).

We therefore conclude that the de novo pathway is the predominant pathway of ceramide accumulation in the light-stressed retina and that this accumulation occurs before the induction of active apoptosis, suggesting a probable causal role of this accumulated ceramide in activating photoreceptor apoptosis in this model. Thus, blocking of this pathway experimentally would be predicted to reduce photoreceptor cell death in LIRD.

De novo ceramide biosynthetic inhibitor FTY720 reduces the light-induced increase in retinal ceramide

FTY720, a recently discovered inhibitor of ceramide synthase (35, 36), is safe, crosses the blood-brain barrier, and has been tested up to a maximum dose of 5 mg/kg/day in humans (30–32, 40). We administered a single dose of FTY720 at 10 mg/kg to Sprague-Dawley rats intraperitoneally 0.5 h before light damage and measured the retinal free ceramide content (C16+C18+C24) by GC-MS at 6 h after light damage. Light stress increased ceramide levels by 2-fold in vehicle-treated retinas (**Fig. 4A**), similar to the results obtained from untreated light-stressed retinas (Fig. 1). However, FYT720 administration significantly blocked the increase in free ceramide levels in the retina (Fig. 4A). The more-sensitive method of ESI-MS/MS revealed similar changes in total ceramide content along with reductions in dihydroceramide and dh-Sph levels (Fig. 4B). These data indicate that FTY720 indeed can act as a de novo ceramide biosynthesis inhibitor in the in vivo retina, and vehicle (50% DMSO) has no effect on retinal ceramide metabolism in relation to light stress (Figs. 1, 3, 4).

FTY720 protects retina from light-induced degeneration

We further tested the effect of FTY720-mediated reduction in ceramide content in the light-stressed retina. Because human clinical trials used a dose of 1 to 5 mg/kg of FTY720/day, we tested three single doses (2.5, 5.0, and 10.0 mg/kg) by intraperitoneal injection at 0.5 h before the start of light exposure. FTY720 treatment preserved rod a-wave responses in a dose-dependent manner, with a dose of 10 mg/kg providing maximal protection (**Fig. 5A**; data for 5.0 mg/kg are not shown). Rod b-wave responses were completely preserved by 10 mg/kg FTY720 to the extent that there was no significant difference between light-damaged and non-light-damaged controls (Fig. 5B). When we administered 2.5 mg/kg at three time points at 16 h before, 0.5 h before, and 0 h after light treatment, we observed 70–80% preservation of rod function (Fig. 5C, D). A single dose of 2.5 mg FTY720 administered 16 h before light treatment was not effective, but 10 mg/kg administered 16 h before light treatment showed slight protection (Fig. 5C, D). However, the same 10 mg/kg at 24 h and 48 h before the exposure to light did not have any protective effect (data not shown). Interestingly, 10 mg/kg FTY720 administered immediately after light damage also could not protect from the retinal functional loss in LIRD (Fig. 5C, D).

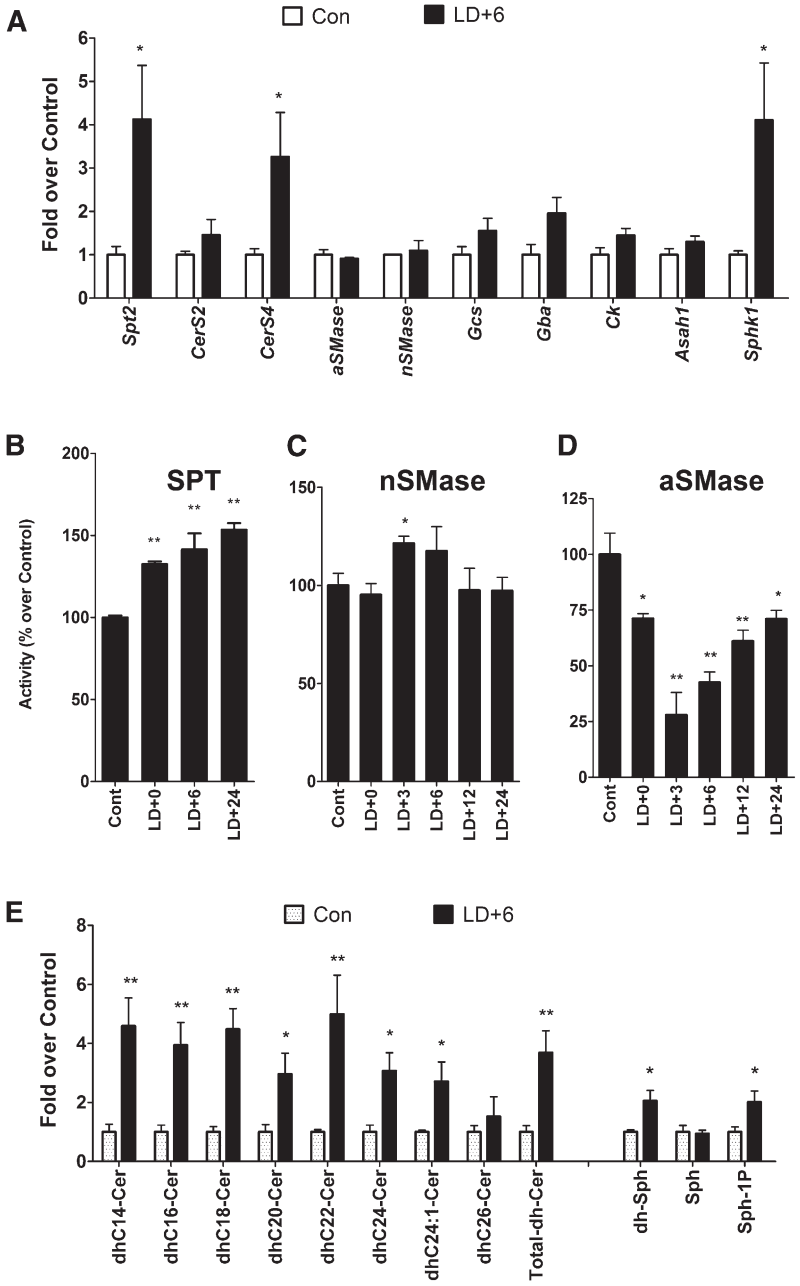

Fig. 3. Pathways of ceramide generation in light-stressed retina. A: Expression of ceramide metabolic genes after light stress. Sprague-Dawley rat retinas were harvested 6 h after light damage (LD+6), and expression data were calculated by delta threshold cycle (dCt) methods after normalizing with three housekeeping genes and presented as fold over Control (Con). (* $P < 0.01$; n = 4–6; Student's *t*-test). Spt, serine palmitoyl transferase; CerS, ceramide synthase; aSMase, acid sphingomyelinase; nSMase, neutral sphingomyelinase; Gcs, glucoceramidesynthase; Gba, glucosidase, β, acid; Ck, ceramide kinase; Asah, acyl-sphingosine amidohydrolases (ceramidases); Sphk, sphingosine kinases. B: SPT activity. The activity of SPT (pmol of product formed/min/mg of protein) is presented as fold over no light-damaged control (Cont). (LD+0, LD+6, LD+24 represent samples harvested at 0 h, 6 h, and 24 h after light damage, respectively). (** $P < 0.01$; n = 4; Student's *t*-test). C: nSMase; D: aSMase activity. The activity of nSMase (C) and aSMase (D) is presented as percentage (%) over control (Cont). (LD+0, LD+3, LD+6, LD+12, LD+24 represent samples harvested at 0 h, 3 h, 6 h, 12 h, and 24 h after light damage, respectively). (* $P < 0.1$, ** $P < 0.01$; n = 4; Student's *t*-test). E: ESI-MS/MS measurement of dihydroceramide (dhCer), dihydrosphingosine (dh-Sph), sphingosine (Sph), and sphingosine-1-phosphate (Sph-1P) levels. Levels of various species of dhCer, total levels of dh-Sph, Sph, and Sph-1P were measured in the retina harvested 6 h after light damage (LD) and compared with no light-damaged control (Con). (* $P < 0.01$; ** $P < 0.001$; n = 4; Student's *t*-test).

Representative H and E-stained sections of the retina 7 days after light damage are shown in **Fig. 6A–F**. By 7 days, the dead photoreceptors were cleared by macrophages, and the remaining nuclei in the ONL represent the surviving photoreceptors. In Fig. 6A, C, E, we show representative low-magnification images of vehicle-treated no-light-damaged, light-damaged, and FTY720-treated light-damaged retinas, respectively. The corresponding higher magnification images of the superior-central retina (boxed area), the area that is affected the most in light damage (15, 16, 20, 58, 59), are presented in Fig. 6B, D, F, respectively. Light damage caused significant loss of photoreceptors (number of nuclei in the ONL or ONL thickness) all over the retina and almost a complete loss in the central retina (Fig. 6D, arrow). Treatment of FTY720 (10 mg/kg) 0.5 h before the start of the light damage protected the photoreceptor cells significantly (6F, arrows showing the protected ONL). By quantitative morphometry, we measured the ONL thickness of the entire retina from superior end to inferior end through the vertical meridian and plotted the values as a spider graph (Fig. 6G). We observed a slight thinning in a small region of the superior central retina in rats treated with 10 mg/kg FTY720 (Fig. 6G, FLD-10 in green tracing). The loss of one to two layers of photoreceptors in this small area was not reflected in the full-field ERG responses, which showed complete functional protection (Fig. 5A, B). The three doses of 2.5 mg also showed protection of most of the retina, except for a 30–50% loss of photoreceptor cells in an ~1 mm^2 area of the superior central retina (Fig. 6G, 2.5-FLDx3 in blue tracing). A single dose of 2.5 mg/kg before light exposure (Fig. 6G, FLD-2.5 purple tracing) and 10 mg/kg FTY720 after light exposure (not

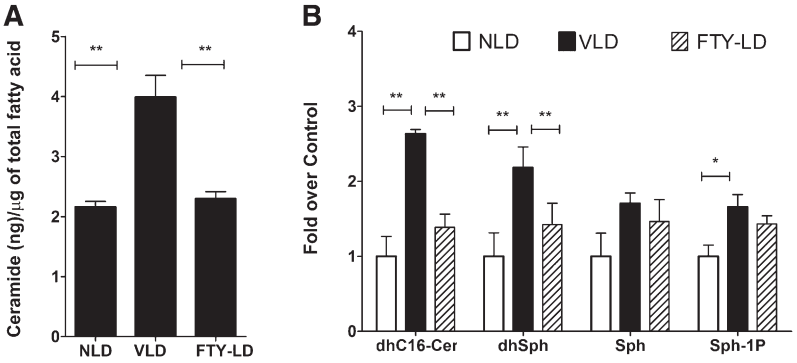

Fig. 4. FTY720 inhibits de novo ceramide biosynthesis in the light-stressed retina. Rat retinas were analyzed for three major species of ceramides (C16, C18, and C24) quantitatively by GC-MS. After removing the free ceramides, the rest of the lipid was analyzed by GC-FID, and the total amount of FA was used to normalize the ceramide values. A: The ceramide level increased significantly in vehicle-treated light-damaged (VLD) rat retinas harvested at 6 h after light damage. Treatment of FTY720 at 10 mg/kg 0.5 h before light damage (FTY-LD) blocked the light-induced ceramide increase in the retina (n = 8; ** $P < 0.001$; Student's *t*-test). B: ESI-MS/MS analysis of dhC16-Cer, dhSph, Sph, and Sph-1P (S1P) in FTY720-treated (FTY-LD) and vehicle-treated light-damaged (VLD) and non light-damaged (NLD) samples (n = 4; * $P < 0.01$; ** $P < 0.001$; Student's *t*-test).

shown) failed to protect against light-induced loss of photoreceptor cells.

In summary, these data showed that FTY720 acted as a de novo ceramide biosynthesis inhibitor in the in vivo retina and reduced the ceramide increase that occurred during light stress. Furthermore, a significant reduction in photoreceptor apoptosis was found after the inhibition of ceramide increase by FTY720. However, FTY720 is also known to have a pleiotropic effect in cellular function and signaling that includes interaction with G-protein-coupled receptors (61, 62). We, therefore, investigated its role in the process of LIRD and in systemic immune suppression, the property for which it is used as multiple sclerosis therapy.

Rhodopsin content and regeneration rate are not affected by FTY720

Activation of rhodopsin, which is a G-protein-coupled receptor, is essential for light-induced rod photoreceptor cell death, and the severity of photodamage depends on the rate of regeneration of the active photopigment (11, 63). Compounds or enzymes that intervene or participate in rhodopsin activation and regeneration are known to modulate the retinal susceptibility to light stress (11, 14, 19). FTY720 can bind and modulate the activity of G-protein-coupled S1P receptors; we, therefore, tested whether FTY720 has any effect on rhodopsin activation and regeneration. In rats maintained in the dark, FTY720 did not cause any changes in the total rhodopsin content when measured 2 h after administration (1.9 ± 0.1 vs. 2.0 ± 0.1 nmol/retina), showing that FTY720 did not directly displace the chromophore from the visual pigment. We then tested whether FTY720 affected the rate of regeneration of functional photopigment by measuring rhodopsin content at several time points before, during, and after a complete photobleach. As indicated in **Fig. 7A**, rhodopsin recovery was not significantly affected by administration of FTY720. FTY720 was administered to fully (overnight) dark-adapted rats that were subsequently exposed to room light for 1 h, which resulted in a complete bleach of rhodopsin in both vehicle- and FTY720-injected rats (Fig. 7A, time = 0 min). When rats were returned to darkness, rhodopsin levels recovered to the dark-adapted level (dotted line, Fig. 7A) by 3 h in both vehicle- and FTY720- treated rats. The rate of recovery of rod photoresponse as measured by ERG in FTY720-treated rats was also not different from the vehicle-treated rats at up to 80 min of dark adaptation (Fig. 7B). Collectively, these results indicate that the protective effects of FTY720 in light damage are not the result of effects on rhodopsin regeneration kinetics or visual cycle activity.

Effect of FTY720 on retinal gene expression

To further understand the effect of FTY720 on light stress-induced retinal changes, we performed gene expression assays by qRT-PCR in retinas harvested 6 h after light damage from the rats treated with 10 mg/kg of FTY720 0.5 h before the start of the 6 h light treatment. FTY720 did not affect the expression of de novo ceramide biosynthetic genes, which were upregulated by light (*Spt2*, *Cers2*, *CerS4*) (**Fig. 8A**). Interestingly, the expression of both acid and neutral SMase genes was induced by 1.5-fold (Fig. 8A). However, FTY720 significantly inhibited the light stress-mediated upregulation of *Sphk1* and *S1P3* genes (Fig. 8B). Induction of *Sphk1* and the receptors of S1P in light-stressed retina could be downstream of ceramide increase, which may explain why their expression goes down when ceramide increase is inhibited by FTY720.

The expression of a number of apoptotic and inflammation-related genes, such as *Fosl1*, *Icam1*, *Ccl2*, *CxCl10*, *Il1b*, and *Il6*, which were upregulated by light stress, was also found to be suppressed significantly in FTY720-treated retinas (Fig. 8C). This also indicates that ceramide action is involved in some of the upstream events for the induction of apoptotic and inflammatory genes in the light-stressed retina, and that is why suppressing its increase suppresses the expression of the downstream genes.

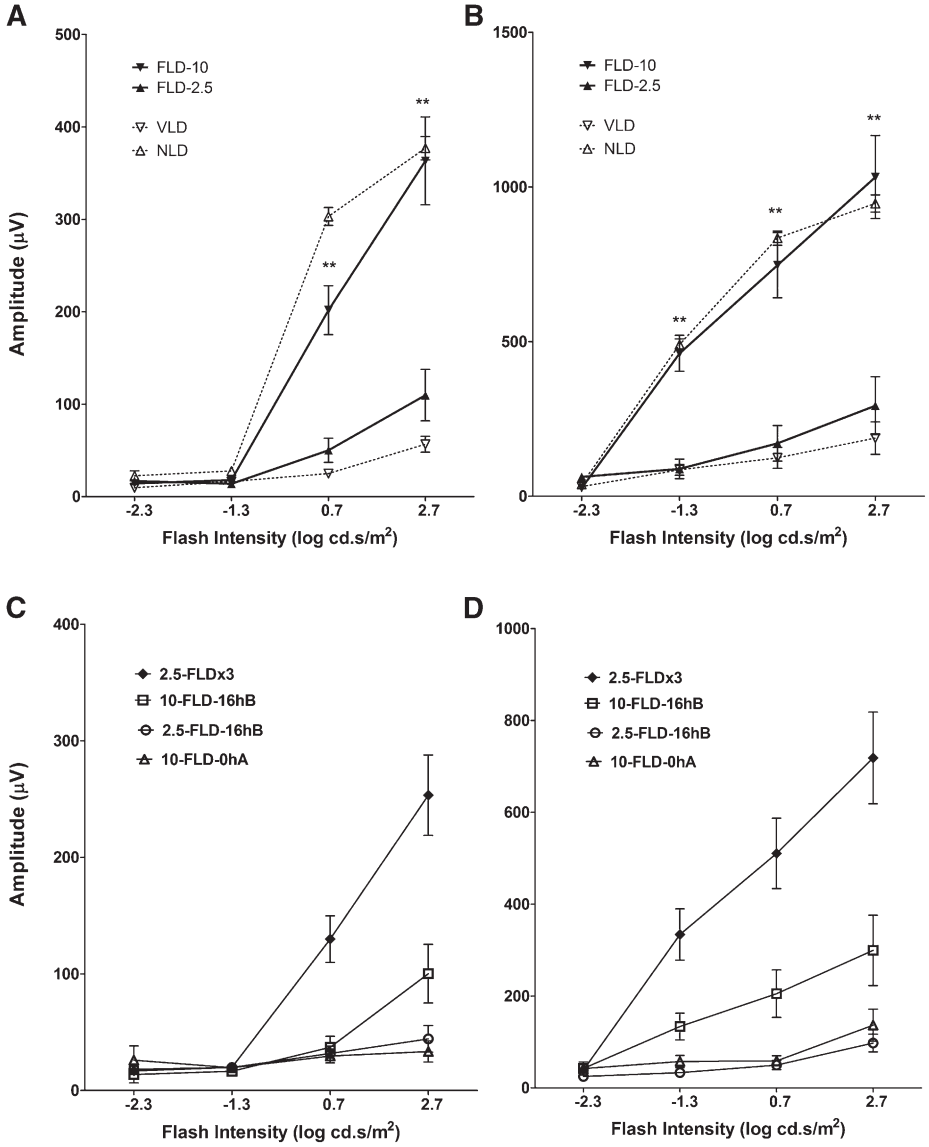

Fig. 5. FTY720 protects rat retinal function: ERG analysis. Scotopic a-wave (A, C) and b-wave (B, D) were measured by light stimulus of increasing flash intensity from -2.3 to 2.7 log cd.s/m^2. A, B: FTY720 administered at different doses 0.5 h before the start of light damage. A dose of 10 mg/kg (FLD-10) of body weight provided >90% protection of the retina but no protection at 2.5 mg/kg (FLD-2.5). C, D: FTY720 administered at different time points before and/or after light damage. When FTY720 was administered at 2.5 mg/kg at three time points (2.5-FLDx3) 16 h before, 0.5 h before, and 0.0 h after light damage, it protected the retina significantly. A single dose of either 2.5 mg or 10.0 mg of FTY720 16 h before light damage (2.5-FLD-16 hB and 10-FLD-16 hB) did not show any protection. FTY720 at 10 mg/kg at 0.0 h after light damage (10-FLD-0 hA) also failed to show any protection (n = 8–10/group; ** $P < 0.001$; Student's *t*-test).

Effect of FTY720 on circulating lymphocytes

FTY720 is approved as a drug for multiple sclerosis for its immunosuppressive properties (34). Systemic FTY720 is phosphorylated to FTY720-P, and as a mimic of S1P, FTY720-P modulates S1P receptor signaling in lymphocyte homing and trafficking. Treatment with FTY720 causes lymphopenia by significantly reducing the number of circulating lymphocytes, which accumulate in the lymph nodes (61, 64, 65). We tested whether suppression of the immune system in the rat may be responsible for protection of retina from light-induced damage by measuring the number of circulating lymphocytes in the peripheral blood after FTY720 treatment. In rats euthanized immediately after light damage, a single dose of FTY720 at 2.5 mg/kg 16 h before the start of light treatment led to a 50% reduction in circulating lymphocytes (**Fig. 9A**). However, this dose of FTY720 could not prevent retinal degeneration (Fig. 5A). A combination of three 2.5 mg/kg doses given at 16 h before, 0.5 h before, and 0.0 h after light damage, and a single 10 mg/kg dose (data not shown) given at 0.5 h before light stress, caused lymphocyte suppression to similar extents (Fig. 9A); however, it had variable effect on retinal protection from LIRD (Fig. 5C, D, 6G; 2.5-FLDx3). The circulating lymphocytes remain suppressed for a week (Fig. 9B),

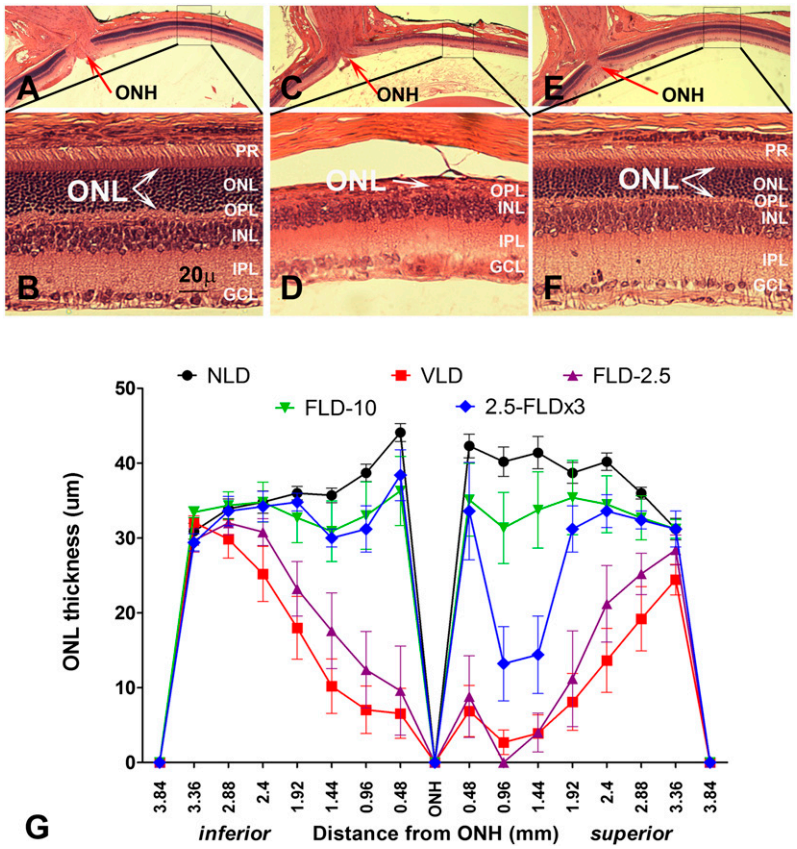

Fig. 6. FTY720 protects rat retinas from LIRD: histological analysis. Representative sections from each treatment: A, B: Vehicle-treated, no light-damaged control; C, D: Vehicle-treated and light-damaged; E, F: FTY720-treated (10 mg/kg) and light-damaged. Portions of the superior central retina (boxed) of Figs. A, C, and E are magnified in Figs. B, D, and F, respectively, and outer nuclear layer (ONL) thickness was demarcated by arrows, which represent the surviving photoreceptor cells. Light damage causes complete loss of photoreceptors (ONL) in this region (D, arrow); however, pretreatment with FTY720 preserved it significantly (Fig.F, arrows). G: Quantitative morphometric measurement of ONL thickness from H and E-stained slides (n = 8–10). NLD, no light-damage; VLD, vehicle-treated and light-damaged; FLD-2.5, single dose of 2.5 mg/kg of FTY720 at 0.5 h before light exposure; FLD-10, single dose of 10 mg/kg of FTY720 at 0.5 h before light exposure; 2.5-FLDx3, FTY720 administered at 2.5 mg/kg at three time points, i.e., 16 h before light damage, 0.5 h before light damage, and 0.0 h after light damage. Abbreviations of retinal layers are defined in Fig. 1.

which does not correlate with retinal protection from light damage, as 10 mg/kg FTY720 at 24 h and 48 h before light stress could not protect the retina.

DISCUSSION

In this study, we found that light stress in the retina increased cellular free ceramides. We also found that this increased ceramide acts as a mediator for photoreceptor apoptosis, because blocking de novo ceramide biosynthesis by administering FTY720 before light stress effectively blocked ceramide increase and preserved retinal structure and function. We determined that the protection of the retina by FTY720 was not related to regeneration kinetics of rhodopsin in light-stressed retina or to the inhibition of lymphocytes in the circulation.

Our study is the first to present direct evidence that ceramide acts as a mediator for LIRD in animal models. LIRD is a very useful model for retinal degeneration research. LIRD models have been used in important discoveries and

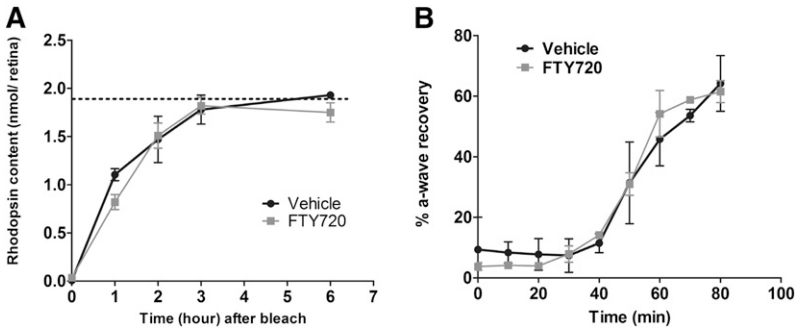

Fig. 7. Effect of FTY720 on visual cycle and rhodopsin regeneration. A: Effect of FTY720 on rhodopsin regeneration. Values represent the mean pmol rhodopsin/retina, and the error bars represent the SE. The horizontal dotted line represents the mean rhodopsin content of fully dark-adapted rats injected with FTY720 or vehicle (n = 4). The curved lines represent the rate of rhodopsin regeneration over time. No significant differences were observed between FTY720-and vehicle-treated rats in their timing to reach a fully dark-adapted state. B: Effect of FTY720 on recovery of rod responses after bleaching measured by ERG. Recovery of rod photoresponses after bleaching (2.3 log cd/m^2 for 2 min) in FTY720- (n = 5) and vehicle-treated (n = 4) rats was shown by percentage of a-wave recovered. FTY720 administration had no significant effect on the recovery of rod responses after bleach.

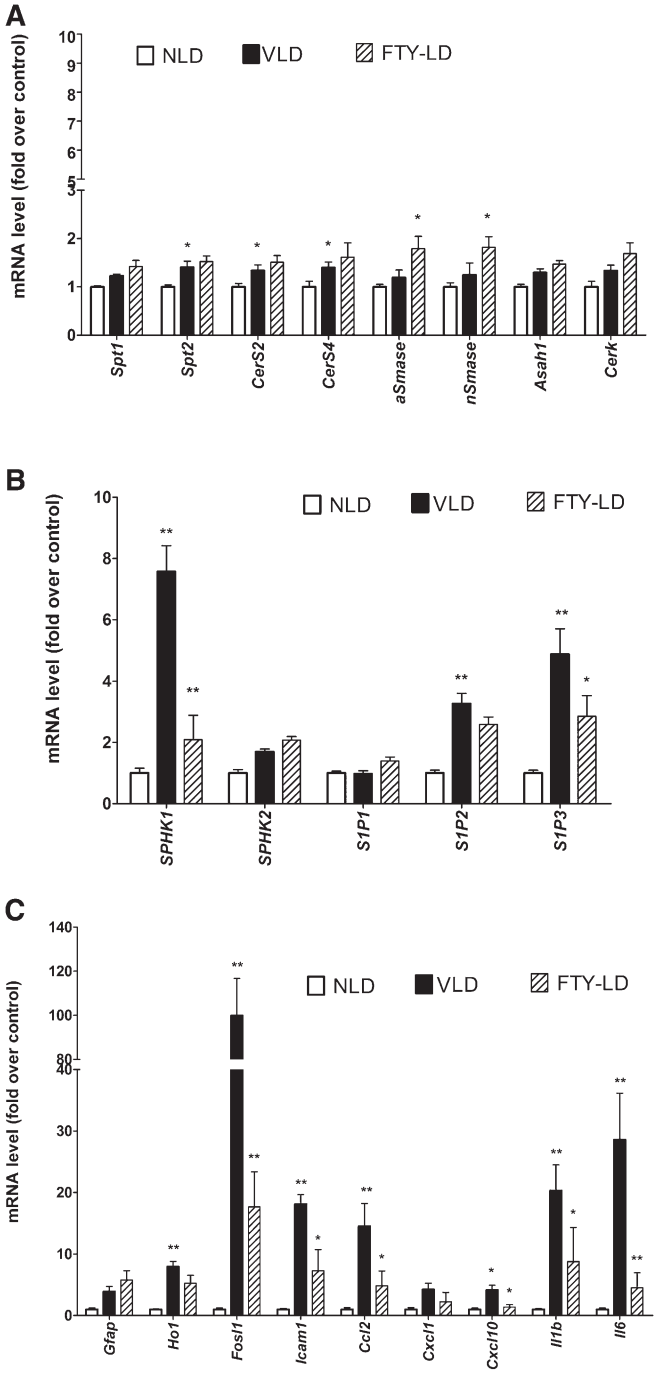

Fig. 8. Effect of FTY720 on retinal gene expression. Retinas were harvested from vehicle-treated no light-damaged (NLD) rats, vehicle-treated light-damaged (VLD) rats, and FTY720-treated light-damaged (FTY-LD) rats 6 h after light damage from all the light-treated rats. Gene expression was measured by qRT-PCR, normalized by using three housekeeping genes (*Rpl19*, *Hgprt*, and *Gapdh*) and presented as a fold over the control group, i.e., NLD. A: Expression of ceramide biosynthetic genes; B: Expression of S1P metabolic and receptor genes; C: Expression of apoptotic and inflammatory genes (n = 4; * $P < 0.1$; ** $P < 0.01$; Student's *t*-test). Full names of the genes are presented in supplementary Table I.

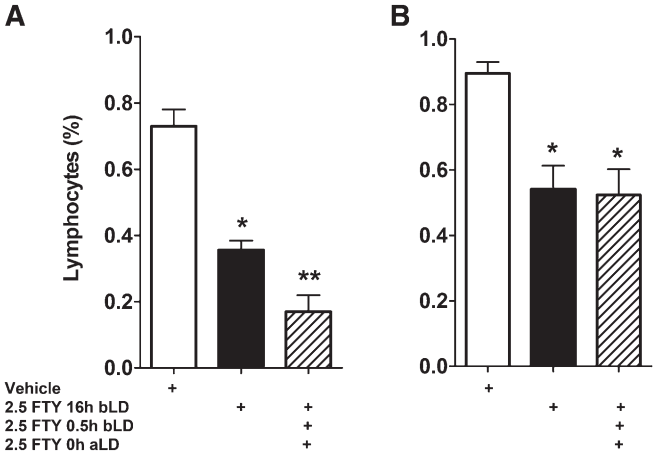

Fig. 9. Effect of FTY720 on circulating lymphocytes. Total white cells were presented as percentage of the numbers of lymphocytes from untreated rats. Blood was drawn and counted immediately at the end of the light damage (A) or 7 days after light damage (B). A: Single (black bar) or triple (patterned bar) dose of FTY720 at 2.5 mg/kg caused a 60–75% reduction of circulating lymphocytes in 6–22 h [6 h when a single dose was administered prior to 6 h-long light damage; 22 h when three doses were administered: the first at 16 h before, the second at 0.5 h before, and the third at 0 h after the 6 h-long light damage. The blood was collected immediately after light damage; therefore, the longest duration of FTY720 treatment was 22 h (16+6)]. B: Both single dose and triple dose of FTY720 could keep the circulating lymphocytes suppressed to ~50% for 7 days, and there were no observed differences between them (n = 5–6; * $P < 0.01$; ** $P < 0.001$; Student's *t*-test; statistical significances are by comparison to the first bar on the left).

have enhanced our understanding of the mechanism of photoreceptor cell death (1–3, 11–14) and the screening of putative neuroprotective compounds (15–21). Retinal degeneration is a heterogeneous group of diseases; mutations in more than 150 genes have already been found for monogenic retinal dystrophies (http://www.sph.uth.tmc.edu/retnet/), the proteins of which are involved in a multitude of structural and functional aspects of photoreceptor, RPE, and other retinal neurons. Therefore, identification of some intermediary metabolite or second messenger that can be targeted for therapies is of great importance. Identification of ceramide as a novel mediator of LIRD will not only aid in other areas of investigations to understand the complex mechanisms of retinal degenerations, but also will serve as a target for therapeutic intervention. In in vitro studies, ceramide produced by the SMase pathway has been shown to induce apoptosis in mouse photoreceptor-derived 661W cells (66). Association of ceramide with apoptosis has also been observed in paraquat-induced cell death of cultured rat retinal neurons (5). In in vivo retinal degeneration studies, ceramide is reported to be the causal agent for inducing photoreceptor apoptosis in mutant models of Drosophila (27), the rd10 mouse model (7), and in a model of rabbit retinal detachment (6). The mechanism by which ceramide induces photoreceptor cell death is therefore an important area of investigation for understanding the complexity of various types of retinal degeneration that are being pursued actively in our current studies. In this present study, we focused on understanding the mechanism of ceramide production in the retina under light stress with an objective of testing the feasibility of targeting a second-messenger-like ceramide in degenerating retina to prevent or delay the progress of degeneration.

Ceramide metabolism is complex, and there could be as many as 200 species of ceramides in a cell (67); there are several pathways that exist for ceramide generation in a cell under various stresses (4). Under light stress, we found the de novo pathway of ceramide generation by activating the first committing enzyme (SPT); ceramide synthases are predominant (Figs. 2, 3), and the major retinal SMase (aSMase) activity was significantly inhibited (Fig. 3D). Because aSMase is the major retinal SMase, we speculated that this cessation of aSMase activity was a cellular autoprotective mechanism to reduce further production of ceramide from sphingomyelin. In pilot studies, we found very limited use of classical de novo ceramide biosynthetic inhibitors such as myriocin and fumonisin B in this rat model of LIRD because of toxicity from systemic administration. We therefore tested FTY720, which was developed from myriocin to reduce its in vivo toxicity and was recently characterized as a ceramide synthase inhibitor (35, 36). In this study, we determined that systemic FTY720 does indeed inhibit ceramide formation in the retina from light-induced stress (Fig. 4), and that the resulting reduction in ceramide levels prevented photoreceptor neurons from cell death (Figs. 5, 6), further confirming the hypothesis that de novo ceramide production mediates retinal degeneration in the LIRD model.

In the past two decades, FTY720, which causes a significant reduction in the number of peripheral blood lymphocytes, has been studied extensively for its potent immunosuppressive activity. As an analog of sphingosine, the mechanism of FTY720 by which it suppresses the immune system is through its phosphorylation to FTY720-phosphate (FTY720-P) by cellular sphingosine kinase, similar to phosphorylation of sphingosine to S1P. As a mimic of S1P, FTY720P can bind to S1P receptors, especially S1P1, on the surface of T lymphocytes. Activation of these receptors determines T-cell egression from the lymph node and migration into the blood, responding to an S1P gradient (61, 62, 68). However, recent findings showed that FTY720 has a pleotropic effect in cell action and signaling, such as inhibiting ceramide synthesis, inhibiting the cannabinoid CB1 receptor, and inhibiting S1P lyase (35, 36, 69, 70).

In our study, we found that the neuroprotective action of FTY720 is different from its systemic immunosuppression effects. In the dose effect study, when we injected FTY720 0.5 h before light exposure, we found a single dose of 2.5 mg/kg had no protection, 5.0 mg/kg had moderate protection, and 10 mg/kg had significant protection of retina from light damage (Fig. 6G); however, inhibition of the circulatory lymphocytes from these three doses showed no differences among them. In rats, FTY720 is known to reduce blood lymphocytes to a minimum level within 3 h after administration; the lymphocytes maintain this minimum level for up to 3 days and slowly recover over a period of 2 weeks (71). It can be deduced that if the suppression of lymphocytes played a role in protecting the retina, then its protective effect should manifest during the period of maximum inhibition of lymphocytes. Although a single dose of 10 mg/kg at 0.5 h before light stress provided the strongest protection (Figs. 5, 6), the same dose at 16 h before light exposure provided only a very slight protection, and at 24 and 48 h before light exposure provided no protection, even though the lymphocytes were still inhibited in all these treatment groups during and after the light stress. Thus, we conclude that the neuroprotective effect of FTY720 is independent of its immunosuppressive effect.

Light signaling started by rhodopsin activation is essential for light-induced rod photoreceptor cell death, and the severity of damage depends on the rate of regeneration of active rhodopsin (11, 63). Therefore, the compounds that interfere with the rhodopsin activation and regeneration process can modulate retinal sensitivity of light stress (15, 19). We found that the rhodopsin-mediated visual cycle was not affected by systemic administration of FTY720 (Fig. 7). However, it is not known whether FTY720P can bind to the S1P receptors present in photoreceptor and RPE cells (Mandal et al., unpublished observations) and affect the visual cycle.

In conclusion, through this study, we found a novel opportunity to target the ceramide synthesis pathway for various human retinal degeneration diseases in which photoreceptor cell death occurs by apoptosis. Our data also suggest that FTY720 and related compounds might be developed as therapeutic drugs for retinal degenerative diseases in which cell death involves ceramide increase. However, in human clinical trials for relapsing MS, FTY720 was found to cause macular edema in 0.5–1.0% of the population. The incidence was higher with higher doses (1.25 vs. 0.5 mg/kg/day) and resolved in 1–6 months after discontinuation of the drug (30, 72). The most-accepted etiology of macular edema is nonspecific inflammation (32, 73, 74). Ceramides and many of their metabolites are well known as inducers of inflammation (75, 76). We now have evidence that FTY720 can modulate ceramide synthesis in the retina (Fig. 4) and we have convincing evidence from unpublished results that an imbalance in the "sphingolipid rheostat," i.e., the regulated balance between ceramide and S1P (77) in the eye, causes retinal inflammation. In healthy retinas, FTY720 may change the ceramide level and thus disturb the sphingolipid rheostat, which in turn causes nonspecific inflammation and macular edema. However, in stressed/degenerating retinas where photoreceptor cells die due to an increase in ceramide levels, FTY720 will still be useful to protect them from degeneration. Ceramide metabolism is complex (67), and FTY720 has pleotropic action; therefore, further studies are needed to determine the effects of FTY720 in stressed retinas as well as in healthy retinas.

Dr. Anisse Saadi, Mark Dittmar, Louisa J. Williams, and Linda S. Boone (from the Department of Ophthalmology, University of Oklahoma Health Sciences Center, Oklahoma City, OK), and Dr. Jacek Bielawski (from the Department of Biochemistry and Molecular Biology, Medical University of South Carolina, Charleston, SC) are gratefully acknowledged by the authors for their provided technical support.

REFERENCES

1. Hao, W., A. Wenzel, M. S. Obin, C. K. Chen, E. Brill, N. V. Krasnoperova, P. Eversole-Cire, Y. Kleyner, A. Taylor, M. I. Simon, et al. 2002. Evidence for two apoptotic pathways in light-induced retinal degeneration. *Nat. Genet.* **32:** 254–260.
2. Remé, C. E., C. Grimm, F. Hafezi, A. Marti, and A. Wenzel. 1998. Apoptotic cell death in retinal degenerations. *Prog. Retin. Eye Res.* **17:** 443–464.
3. Wenzel, A., C. Grimm, M. Samardzija, and C. E. Reme. 2005. Molecular mechanisms of light-induced photoreceptor apoptosis and neuroprotection for retinal degeneration. *Prog. Retin. Eye Res.* **24:** 275–306.
4. Hannun, Y. A., and L. M. Obeid. 2008. Principles of bioactive lipid signalling: lessons from sphingolipids. *Nat. Rev. Mol. Cell Biol.* **9:** 139–150.
5. German, O. L., G. E. Miranda, C. E. Abrahan, and N. P. Rotstein. 2006. Ceramide is a mediator of apoptosis in retina photoreceptors. *Invest. Ophthalmol. Vis. Sci.* **47:** 1658–1668.
6. Ranty, M. L., S. Carpentier, M. Cournot, I. Rico-Lattes, F. Malecaze, T. Levade, M. B. Delisle, and J. C. Quintyn. 2009. Ceramide production associated with retinal apoptosis after retinal detachment. *Graefes Arch. Clin. Exp. Ophthalmol.* **247:** 215–224.
7. Strettoi, E., C. Gargini, E. Novelli, G. Sala, I. Piano, P. Gasco, and R. Ghidoni. 2010. Inhibition of ceramide biosynthesis preserves photoreceptor structure and function in a mouse model of retinitis pigmentosa. *Proc. Natl. Acad. Sci. USA.* **107:** 18706–18711.
8. Zhu, D., P. G. Sreekumar, D. R. Hinton, and R. Kannan. 2010. Expression and regulation of enzymes in the ceramide metabolic pathway in human retinal pigment epithelial cells and their relevance to retinal degeneration. *Vision Res.* **50:** 643–651.
9. Demontis, G. C., B. Longoni, and P. L. Marchiafava. 2002. Molecular steps involved in light-induced oxidative damage to retinal rods. *Invest. Ophthalmol. Vis. Sci.* **43:** 2421–2427.
10. Noell, W. K., V. S. Walker, B. S. Kang, and S. Berman. 1966. Retinal damage by light in rats. *Invest. Ophthalmol.* **5:** 450–473.
11. Grimm, C., A. Wenzel, F. Hafezi, S. Yu, T. M. Redmond, and C. E. Reme. 2000. Protection of Rpe65-deficient mice identifies rhodopsin as a mediator of light-induced retinal degeneration. *Nat. Genet.* **25:** 63–66.
12. Marc, R. E., B. W. Jones, C. B. Watt, F. Vazquez-Chona, D. K. Vaughan, and D. T. Organisciak. 2008. Extreme retinal remodeling triggered by light damage: implications for age related macular degeneration. *Mol. Vis.* **14:** 782–806.
13. Organisciak, D. T., and D. K. Vaughan. 2010. Retinal light damage: mechanisms and protection. *Prog. Retin. Eye Res.* **29:** 113–134.
14. Wenzel, A., C. E. Reme, T. P. Williams, F. Hafezi, and C. Grimm. 2001. The Rpe65 Leu450Met variation increases retinal resistance against light-induced degeneration by slowing rhodopsin regeneration. *J. Neurosci.* **21:** 53–58.
15. Mandal, M. N., G. P. Moiseyev, M. H. Elliott, A. Kasus-Jacobi, X. Li, H. Chen, L. Zheng, O. Nikolaeva, R. A. Floyd, J. X. Ma, et al. 2011. Alpha-phenyl-N-tert-butylnitrone (PBN) prevents light-induced degeneration of the retina by inhibiting RPE65 protein isomerohydrolase activity. *J. Biol. Chem.* **286:** 32491–32501.
16. Mandal, M. N., J. M. Patlolla, L. Zheng, M. P. Agbaga, J. T. Tran, L. Wicker, A. Kasus-Jacobi, M. H. Elliott, C. V. Rao, and R. E. Anderson. 2009. Curcumin protects retinal cells from light-and oxidant stress-induced cell death. *Free Radic. Biol. Med.* **46:** 672–679.
17. Organisciak, D. T., H. M. Wang, Z. Y. Li, and M. O. Tso. 1985. The protective effect of ascorbate in retinal light damage of rats. *Invest. Ophthalmol. Vis. Sci.* **26:** 1580–1588.
18. Ranchon, I., S. Chen, K. Alvarez, and R. E. Anderson. 2001. Systemic administration of phenyl-N-tert-butylnitrone protects the retina from light damage. *Invest. Ophthalmol. Vis. Sci.* **42:** 1375–1379.
19. Sieving, P. A., P. Chaudhry, M. Kondo, M. Provenzano, D. Wu, T. J. Carlson, R. A. Bush, and D. A. Thompson. 2001. Inhibition of the visual cycle in vivo by 13-cis retinoic acid protects from light damage and provides a mechanism for night blindness in isotretinoin therapy. *Proc. Natl. Acad. Sci. USA.* **98:** 1835–1840.
20. Tanito, M., F. Li, M. H. Elliott, M. Dittmar, and R. E. Anderson. 2007. Protective effect of TEMPOL derivatives against light-induced retinal damage in rats. *Invest. Ophthalmol. Vis. Sci.* **48:** 1900–1905.
21. Tanito, M., H. Masutani, Y. C. Kim, M. Nishikawa, A. Ohira, and J. Yodoi. 2005. Sulforaphane induces thioredoxin through the antioxidant-responsive element and attenuates retinal light damage in mice. *Invest. Ophthalmol. Vis. Sci.* **46:** 979–987.
22. Hannun, Y. A. 1996. Functions of ceramide in coordinating cellular responses to stress. *Science.* **274:** 1855–1859.
23. Arboleda, G., L. C. Morales, B. Benitez, and H. Arboleda. 2009. Regulation of ceramide-induced neuronal death: cell metabolism meets neurodegeneration. *Brain Res. Rev.* **59:** 333–346.
24. Petrache, I., V. Natarajan, L. Zhen, T. R. Medler, A. T. Richter, C. Cho, W. C. Hubbard, E. V. Berdyshev, and R. M. Tuder. 2005. Ceramide upregulation causes pulmonary cell apoptosis and emphysema-like disease in mice. *Nat. Med.* **11:** 491–498.
25. Obeid, L. M., C. M. Linardic, L. A. Karolak, and Y. A. Hannun. 1993. Programmed cell death induced by ceramide. *Science.* **259:** 1769–1771.
26. Nikolova-Karakashian, M. N., and K. A. Rozenova. 2010. Ceramide in stress response. *Adv. Exp. Med. Biol.* **688:** 86–108.
27. Acharya, U., S. Patel, E. Koundakjian, K. Nagashima, X. Han, and J. K. Acharya. 2003. Modulating sphingolipid biosynthetic pathway rescues photoreceptor degeneration. *Science.* **299:** 1740–1743.
28. Zhang, Z., and H. J. Schluesener. 2007. FTY720: a most promising immunosuppressant modulating immune cell functions. *Mini Rev. Med. Chem.* **7:** 845–850.
29. Brinkmann, V. 2009. FTY720 (fingolimod) in multiple sclerosis: therapeutic effects in the immune and the central nervous system. *Br. J. Pharmacol.* **158:** 1173–1182.
30. Cohen, J. A., F. Barkhof, G. Comi, H. P. Hartung, B. O. Khatri, X. Montalban, J. Pelletier, R. Capra, P. Gallo, G. Izquierdo, et al. 2010. Oral fingolimod or intramuscular interferon for relapsing multiple sclerosis. *N. Engl. J. Med.* **362:** 402–415.
31. Kappos, L., J. Antel, G. Comi, X. Montalban, P. O'Connor, C. H. Polman, T. Haas, A. A. Korn, G. Karlsson, and E. W. Radue. 2006. Oral fingolimod (FTY720) for relapsing multiple sclerosis. *N. Engl. J. Med.* **355:** 1124–1140.
32. Kappos, L., E. W. Radue, P. O'Connor, C. Polman, R. Hohlfeld, P. Calabresi, K. Selmaj, C. Agoropoulou, M. Leyk, L. Zhang-Auberson, et al. 2010. A placebo-controlled trial of oral fingolimod in relapsing multiple sclerosis. *N. Engl. J. Med.* **362:** 387–401.
33. Mansoor, M., and A. J. Melendez. 2008. Recent trials for FTY720 (fingolimod): a new generation of immunomodulators structurally similar to sphingosine. *Rev. Recent Clin. Trials.* **3:** 62–69.
34. Schwab, S. R., and J. G. Cyster. 2007. Finding a way out: lymphocyte egress from lymphoid organs. *Nat. Immunol.* **8:** 1295–1301.
35. Berdyshev, E. V., I. Gorshkova, A. Skobeleva, R. Bittman, X. Lu, S. M. Dudek, T. Mirzapoiazova, J. G. Garcia, and V. Natarajan. 2009. FTY720 inhibits ceramide synthases and up-regulates dihydrosphingosine 1-phosphate formation in human lung endothelial cells. *J. Biol. Chem.* **284:** 5467–5477.
36. Lahiri, S., H. Park, E. L. Laviad, X. Lu, R. Bittman, and A. H. Futerman. 2009. Ceramide synthesis is modulated by the sphingosine analog FTY720 via a mixture of uncompetitive and noncompetitive inhibition in an acyl-CoA chain length-dependent manner. *J. Biol. Chem.* **284:** 16090–16098.
37. Commodaro, A. G., J. P. Peron, C. T. Lopes, C. Arslanian, R. Belfort, Jr., L. V. Rizzo, and V. Bueno. 2010. Evaluation of experimental autoimmune uveitis in mice treated with FTY720. *Invest. Ophthalmol. Vis. Sci.* **51:** 2568–2574.
38. Kurose, S., E. Ikeda, M. Tokiwa, N. Hikita, and M. Mochizuki. 2000. Effects of FTY720, a novel immunosuppressant, on experimental autoimmune uveoretinitis in rats. *Exp. Eye Res.* **70:** 7–15.
39. Raveney, B. J., D. A. Copland, L. B. Nicholson, and A. D. Dick. 2008. Fingolimod (FTY720) as an acute rescue therapy for intraocular inflammatory disease. *Arch. Ophthalmol.* **126:** 1390–1395.
40. Meno-Tetang, G. M., H. Li, S. Mis, N. Pyszczynski, P. Heining, P. Lowe, and W. J. Jusko. 2006. Physiologically based pharmacokinetic modeling of FTY720 (2-amino-2[2-(-4-octylphenyl)ethyl]propane-1,3-diol hydrochloride) in rats after oral and intravenous doses. *Drug Metab. Dispos.* **34:** 1480–1487.
41. Winkler, B. S. 1972. The electroretinogram of the isolated rat retina. *Vision Res.* **12:** 1183–1198.
42. Tanito, M., R. S. Brush, M. H. Elliott, L. D. Wicker, K. R. Henry, and R. E. Anderson. 2009. High levels of retinal membrane docosahexaenoic acid increase susceptibility to stress-induced degeneration. *J. Lipid Res.* **50:** 807–819.
43. Irreverre, F., A. L. Stone, H. Shichi, and M. S. Lewis. 1969. Biochemistry of visual pigments. I. Purification and properties of bovine rhodopsin. *J. Biol. Chem.* **244:** 529–536.

44. Zhang, Y., P. Mattjus, P. C. Schmid, Z. Dong, S. Zhong, W. Y. Ma, R. E. Brown, A. M. Bode, H. H. Schmid, and Z. Dong. 2001. Involvement of the acid sphingomyelinase pathway in uva-induced apoptosis. *J. Biol. Chem.* **276:** 11775–11782.
45. Brush, R. S., J. T. Tran, K. R. Henry, M. E. McClellan, M. H. Elliott, and M. N. Mandal. 2010. Retinal sphingolipids and their very-long-chain fatty acid-containing species. *Invest. Ophthalmol. Vis. Sci.* **51:** 4422–4431.
46. Martin, R. E., M. H. Elliott, R. S. Brush, and R. E. Anderson. 2005. Detailed characterization of the lipid composition of detergent-resistant membranes from photoreceptor rod outer segment membranes. *Invest. Ophthalmol. Vis. Sci.* **46:** 1147–1154.
47. Bielawski, J., Z. M. Szulc, Y. A. Hannun, and A. Bielawska. 2006. Simultaneous quantitative analysis of bioactive sphingolipids by high-performance liquid chromatography-tandem mass spectrometry. *Methods.* **39:** 82–91.
48. Mandal, M. N., R. Ambasudhan, P. W. Wong, P. J. Gage, P. A. Sieving, and R. Ayyagari. 2004. Characterization of mouse orthologue of ELOVL4: genomic organization and spatial and temporal expression. *Genomics.* **83:** 626–635.
49. Mandal, M. N., and R. Ayyagari. 2006. Complement factor H: spatial and temporal expression and localization in the eye. *Invest. Ophthalmol. Vis. Sci.* **47:** 4091–4097.
50. Mandal, M. N., V. Vasireddy, M. M. Jablonski, X. Wang, J. R. Heckenlively, B. A. Hughes, G. B. Reddy, and R. Ayyagari. 2006. Spatial and temporal expression of MFRP and its interaction with CTRP5. *Invest. Ophthalmol. Vis. Sci.* **47:** 5514–5521.
51. Mandal, M. N., V. Vasireddy, G. B. Reddy, X. Wang, S. E. Moroi, B. R. Pattnaik, B. A. Hughes, J. R. Heckenlively, P. F. Hitchcock, M. M. Jablonski, et al. 2006. CTRP5 is a membrane-associated and secretory protein in the RPE and ciliary body and the S163R mutation of CTRP5 impairs its secretion. *Invest. Ophthalmol. Vis. Sci.* **47:** 5505–5513.
52. Sherry, D. M., R. Mitchell, H. Li, D. R. Graham, and J. D. Ash. 2005. Leukemia inhibitory factor inhibits neuronal development and disrupts synaptic organization in the mouse retina. *J. Neurosci. Res.* **82:** 316–332.
53. Williams, R. D., E. Wang, and A. H. Merrill, Jr. 1984. Enzymology of long-chain base synthesis by liver: characterization of serine palmitoyltransferase in rat liver microsomes. *Arch. Biochem. Biophys.* **228:** 282–291.
54. Dickson, R. C., R. L. Lester, and M. M. Nagiec. 2000. Serine palmitoyltransferase. *Methods Enzymol.* **311:** 3–9.
55. Noell, W. K., and R. Albrecht. 1971. Irreversible effects on visible light on the retina: role of vitamin A. *Science.* **172:** 76–79.
56. Hafezi, F., A. Marti, K. Munz, and C. E. Reme. 1997. Light-induced apoptosis: differential timing in the retina and pigment epithelium. *Exp. Eye Res.* **64:** 963–970.
57. Gordon, W. C., D. M. Casey, W. J. Lukiw, and N. G. Bazan. 2002. DNA damage and repair in light-induced photoreceptor degeneration. *Invest. Ophthalmol. Vis. Sci.* **43:** 3511–3521.
58. Tanito, M., M. H. Elliott, Y. Kotake, and R. E. Anderson. 2005. Protein modifications by 4-hydroxynonenal and 4-hydroxyhexenal in light-exposed rat retina. *Invest. Ophthalmol. Vis. Sci.* **46:** 3859–3868.
59. Tanito, M., S. Kaidzu, A. Ohira, and R. E. Anderson. 2008. Topography of retinal damage in light-exposed albino rats. *Exp. Eye Res.* **87:** 292–295.
60. Ogretmen, B., and Y. A. Hannun. 2004. Biologically active sphingolipids in cancer pathogenesis and treatment. *Nat. Rev Cancer.* **4:** 604–616.
61. Aktas, O., P. Kury, B. Kieseier, and H. P. Hartung. 2010. Fingolimod is a potential novel therapy for multiple sclerosis. *Nat. Rev. Neurol.* **6:** 373–382.
62. Gräler, M. H. 2010. Targeting sphingosine 1-phosphate (S1P) levels and S1P receptor functions for therapeutic immune interventions. *Cell. Physiol. Biochem.* **26:** 79–86.
63. Humphries, M. M., D. Rancourt, G. J. Farrar, P. Kenna, M. Hazel, R. A. Bush, P. A. Sieving, D. M. Sheils, N. McNally, P. Creighton, et al. 1997. Retinopathy induced in mice by targeted disruption of the rhodopsin gene. *Nat. Genet.* **15:** 216–219.
64. Edmonds, Y., S. Milstien, and S. Spiegel. 2011. Development of small-molecule inhibitors of sphingosine-1-phosphate signaling. *Pharmacol. Ther.* **132:** 352–360.
65. Zemann, B., B. Kinzel, M. Muller, R. Reuschel, D. Mechtcheriakova, N. Urtz, F. Bornancin, T. Baumruker, and A. Billich. 2006. Sphingosine kinase type 2 is essential for lymphopenia induced by the immunomodulatory drug FTY720. *Blood.* **107:** 1454–1458.
66. Sanvicens, N., and T. G. Cotter. 2006. Ceramide is the key mediator of oxidative stress-induced apoptosis in retinal photoreceptor cells. *J. Neurochem.* **98:** 1432–1444.
67. Cho, J. H., W. H. Klein, and M. J. Tsai. 2007. Compensational regulation of bHLH transcription factors in the postnatal development of BETA2/NeuroD1-null retina. *Mech. Dev.* **124:** 543–550.
68. Walter, S., and K. Fassbender. 2010. Spingolipids in multiple sclerosis. *Cell. Physiol. Biochem.* **26:** 49–56.
69. Paugh, S. W., M. P. Cassidy, H. He, S. Milstien, L. J. Sim-Selley, S. Spiegel, and D. E. Selley. 2006. Sphingosine and its analog, the immunosuppressant 2-amino-2-(2-[4-octylphenyl]ethyl)-1,3-propanediol, interact with the CB1 cannabinoid receptor. *Mol. Pharmacol.* **70:** 41–50.
70. Bandhuvula, P., Y. Y. Tam, B. Oskouian, and J. D. Saba. 2005. The immune modulator FTY720 inhibits sphingosine-1-phosphate lyase activity. *J. Biol. Chem.* **280:** 33697–33700.
71. Suzuki, S., S. Enosawa, T. Kakefuda, T. Shinomiya, M. Amari, S. Naoe, Y. Hoshino, and K. Chiba. 1996. A novel immunosuppressant, FTY720, with a unique mechanism of action, induces long-term graft acceptance in rat and dog allotransplantation. *Transplantation.* **61:** 200–205.
72. Rajesh, M., A. Kolmakova, and S. Chatterjee. 2005. Novel role of lactosylceramide in vascular endothelial growth factor-mediated angiogenesis in human endothelial cells. *Circ. Res.* **97:** 796–804.
73. Perrotta, C., and E. Clementi. 2010. Biological roles of acid and neutral sphingomyelinases and their regulation by nitric oxide. *Physiology (Bethesda).* **25:** 64–71.
74. Andrieu-Abadie, N., V. Gouaze, R. Salvayre, and T. Levade. 2001. Ceramide in apoptosis signaling: relationship with oxidative stress. *Free Radic. Biol. Med.* **31:** 717–728.
75. Nixon, G. F. 2009. Sphingolipids in inflammation: pathological implications and potential therapeutic targets. *Br. J. Pharmacol.* **158:** 982–993.
76. Pettus, B. J., C. E. Chalfant, and Y. A. Hannun. 2004. Sphingolipids in inflammation: roles and implications. *Curr. Mol. Med.* **4:** 405–418.
77. Spiegel, S., and S. Milstien. 2003. Sphingosine-1-phosphate: an enigmatic signalling lipid. *Nat. Rev Mol. Cell. Biol.* **4:** 397–407.